

# Analysis and simulation of non-metallic inclusions in spheroidal graphite iron

**B Pustal<sup>a</sup>, B Schelberger and A Bührig-Polaczek**

Foundry Institute at RWTH Aachen University, Intzestr. 5, 52072 Aachen, Germany

E-mail: <sup>a</sup>b.pustal@gi.rwth-aachen.de

**Abstract.** Non-metallic inclusions in spheroidal cast iron (SGI) reduce fatigue strength and yield strength. This type of inclusion usually accumulates at grain boundaries. Papers addressing this topic show the overall impact of both the fraction of so-called white (carbides) and black (non-metallic) inclusions on mechanical properties. In the present work we focus on the origin and the formation conditions of black Mg-bearing inclusions, further distinguishing between Si-bearing and non-Si-bearing Mg inclusions. The formation was simulated applying thermodynamic approaches. Moreover, appropriate experiments have been carried out and a large number of particles have been studied applying innovative feature analysis with regard to shape, size, and composition. Magnesium silicates are predicted at elevated oxygen concentrations, whereas at low levels of oxygen sulphides and carbides appear at a late stage of solidification. Experiments with three consecutive flow obstacles show that the amount of magnesium silicates decrease after each of the three obstacles, whereas the fraction of non-Si-bearing inclusions remains approximately constant. The size of inclusions divides in halves over the flow path and the number of particles increases accordingly. We point out that based on feature analysis Mg-O-C bearing inclusion show disadvantageous form factors for which reason this kind of inclusions may be extremely harmful in terms of crack initiation. All results obtained indicate that magnesium silicates are entrapped on mould filling, whereas Mg-(O, C, S, P, N) bearing particles are precipitates at late stages of solidification. Consequently, the only avoidance strategy is setting up optimum retained magnesium content.

## 1. Introduction

Non-metallic inclusions decrease fatigue strength and yield strength of SGI, since they accumulate near grain boundaries. This weakening notch effect in the matrix structure is severe if caused by a jagged or worm-like morphology of these inclusions. Papers addressing this topic show the overall impact of both the fraction of so-called white (carbides) and black (non-metallic) inclusions on mechanical properties. The cause for the formation of these inclusions and the associated morphology is not yet sufficiently known. After the magnesium treatment of the cast iron melt for the production of spheroidal graphite iron (SGI) small amounts of oxygen, sulphur, magnesium, and other trace elements will remain in the melt. These elements form silicates on the one hand, and on the other hand the solubility of these elements in the austenite is usually very low, which causes microsegregation. At a sufficiently high concentration of these elements in the residual melt, Mg-bearing precipitates are expected. One aim of the present study was to determine the thermodynamic conditions under which such inclusions occur. Furthermore, two hypotheses were followed: the inclusion hypothesis after which such inclusions form before or during mold filling, and the precipitation hypothesis that non-metallic precipitations occur towards the end of solidification in the residual melt areas. Supplementary experiments were conducted to support these theses, or to refute them.



## 2. State of the art

Sofue et al. [1] investigated the influence of grain size, graphite shape, amount of non-metallic inclusions, matrix structure and matrix hardness on the fatigue strength. Their results show that the graphite roundness increases steadily with the remaining magnesium content, but also the number of non-metallic inclusions. The weakening of the grain boundaries through non-metallic inclusions exceeds the effect of the spheroid roundness at about 0.6 wt.- % retained magnesium. Beyond this point, elongation and fatigue strength decrease again. Sofue et al. created rules for the production of high quality SGI with improved fatigue strength on the basis of their results. They divided non-metallic inclusions into white (Ti, Cr carbides) and black Mg-bearing inclusions. They noted that the detailed composition of these inclusions has not been adequately characterized. Using electrolytic etching and EDX, Hiroshi et al. [2] investigated the three-dimensional shape and composition of various inclusions, thereby distinguishing titanium phosphides, Ti (C, N), and non-metallic inclusions from the Mg-Al-Si-O and Ti-C-Si-P-S systems. In their work with high silicon cast iron, Lin et al. [3] pointed out, that the presence of magnesium inclusions initiates cracks at the cell boundaries under cyclic load.

Thermodynamic calculations on the phase structure of steel materials are state of the art for many applications [4] and [5]. In optimization of cast iron materials, however, such a methodology is still the exception [6]. The software Thermo-Calc [7] or FactSage [8] are capable of performing thermodynamic calculations with multicomponent systems. From the thermodynamic data, such as enthalpy, entropy, and heat capacity, the solidification behaviour can also be derived [7]. With this method, effects of individual elements on the amount of non-metallic inclusions depending on the temperature were determined [9]. The main kinetic factors influencing cell distances based on the nucleation or diffusion in the austenite shell cannot be calculated with thermodynamic methods alone. This can only be achieved by means of kinetic models such as the microsegregation model of Pustal et al. [10]. The continued segregation of the alloying elements on the basis of thermodynamic and mobility data and the formation of related precipitates is numerically calculated. In this model simulation of the solidification and diffusion occurs along an axis that reflects a characteristic length, depending on the assumed morphology. In dendritic growth this length corresponds to half the dendrite arm spacing. In a eutectic cell, this axis corresponds to the half distance between the graphite nuclei. The species transport problem of all alloying elements can be solved in several solid phases, and for the thermodynamic equilibrium calculations at the phase boundary, the tq-interface of Thermo-Calc [7] is used. The model takes into account the mobility of the elements as well as their interaction during segregation. For example, up-hill diffusion of carbon can be predicted. These effects influence the solidification behavior of SGI considerably.

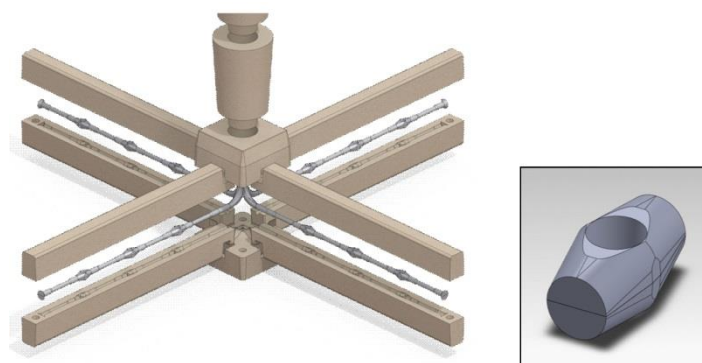


**Figure 1.** Quadruple mold with arrangement of three flow obstacles in each of the four arms (left) and cylindrical obstacle geometry (right).

### 3. Work carried out

#### 3.1. Casting

To quantify the influence of mold filling on the amount and type of non-metallic inclusions, an experiment was set up, that allows generating such inclusions in flow obstacles. The mold in figure 1, designated as “quadrupel test”, has been successfully used for the selective generation of oxide inclusions in magnesium casting.

The modular mold is assembled of individual cold-box cores, the down sprue through which the pouring height can be varied, the gating element at the base, and four horizontal arms, which represent the actual casting. In each arm up to three flow obstacles can be inserted at regular intervals. During mold filling eddies form in the flow shadow of the flow obstacle. These in turn lead to increased contact between melt and atmosphere, so that an increased possibility for the formation of oxides exists, where appropriate reactants are present. If turbulent mold filling has significant influence on the formation of Mg inclusions, then their amount should increase in the casting behind the obstacles along the flow path.

We further subdivided the inclusions in Si-bearing and non-Si-bearing Mg inclusions. Key research questions of casting trials were whether an increase of Mg-bearing inclusions along the flow path is taking place, and whether the proportion of finely divided non-Si-bearing inclusion behaves in the same manner as the amount of Si-bearing particles. If the amounts of non-Si-bearing inclusions along the flow path develop in the same or similar manner as the amounts of Si-bearing inclusions, then this would be an indication of an influence of the mold filling conditions on non-Si-bearing particle formation. But, if the non-Si-bearing inclusions are equally distributed, while magnesium silicates increase, then the influence of mold filling on the non-Si-bearing inclusions is secondary and non-Si-bearing inclusions are precipitates. For this purpose, a sample was taken after each flow obstacle, ground, and polished for analysis.

#### 3.2. Analysis

For identification of inclusions or precipitates, scanning electron microscopy (SEM) was used. Due to the small size of the particles a so-called feature analysis was applied instead of conventional image analysis. In this method, image analysis is conducted on the basis of automatically generated SEM images over a large sample area. Subsequently, all characteristic particles are automatically checked with EDX measurement. In this way, a record was created for each particle to the entire measurement area of about 0.38 mm<sup>2</sup> containing size, composition, shape, and surface area. Because of this highly time-consuming procedure, this process could be performed for only three samples at one arm.

#### 3.3. Thermodynamic / thermodynamic-kinetic simulations

For the thermodynamic calculations the software FactSage [8] along with the databases FStel and Ftoxid [8] were applied. Calculations were performed at thermodynamic equilibrium and according to the Gulliver-Scheil model, that is, no diffusion in the solid state, infinite rapid diffusion in the liquid phase. As a starting point for variations of oxygen the composition C3.45 Si2.19 Mn0.14 P0.018 S0.006 Mg0.028 wt.-% was selected. The oxygen content was varied between 19 ppm and 0.1 wt.-% and the effect of the presence or absence of sulphur in the melt during the development of Mg-bearing precipitates was taken into account. The results of this study are given in Section 4.2.

Applying the microsegregation software microphase along with the database Iron-01c, both described in Pustal et al. [10], simulations were performed with the initial compositions Fe C3.62 Si2.4 Mn0.08 wt.-% and variation of the retained Mg: 0.02, 0.04, 0.08 wt.-%. In each such case the resulting residual melt concentration at 1 wt.-% liquid was calculated as: C3.96 Mn0.29 Si1.21 wt.-% and Mg: 0.21, 0.43, 0.87 wt.-%. These concentrations represent the conditions in the intercellular residual melt areas where non-metallic inclusions were found. These conditions were then applied in FactSage as initial concentration for calculating compounds at thermodynamic equilibrium. The

calculations were carried out at temperatures between 1000 °C and 1400 °C with the addition of 19 ppm of oxygen and the final results of this procedure are shown in Section 4.2.

## 4. Results

### 4.1. Results of analysis

Feature analysis was conducted at three samples taken behind each of the three flow obstacles of one arm, to determine the statistical change in the number of particles, the particle size, and the area ratio for the different kinds of particles bearing Mg with and without Si. Figure 2 (a) shows that both types of particles are present in roughly equal amounts in the microstructure. The area ratio of all Mg-bearing particles decreases after each flow obstacle. This is mainly due to the decrease of magnesium silicates, since the amount of Mg (O, C, S, P, N)-bearing particles without Si remains approximately constant. The discrepancies at sample position 2 are due to porosity at this location which impacts the acquisition of the values measured. When neglecting sample position 2, the drawn trend of decrease or increase remains. Figure 2 (b) shows that the particles behind the first flow obstacle are large with an average of about  $1.5 \mu\text{m}^2$ , whereas behind the third module these particles are small; the mean area is only about  $0.65 \mu\text{m}^2$ . Along with the particle size, the particle density ( $n\text{-particles}/100\mu\text{m}^2$ ) decreases. The form factor decreases strongly, that is, the particle roundness improved considerably over the sample position. This means, that after the first flow obstacle a few large and rather jagged particles occur and behind the last module, there are many more small rounded particles. In a further differentiation, it was found that the non-Si-bearing particles decrease in size more noticeably, whereas the form factor improvement is more pronounced in the Si-bearing particles. It can be concluded that the non-Si-bearing particles due to their size and disadvantageous shape may impact the mechanical properties more than the Si-bearing inclusions.

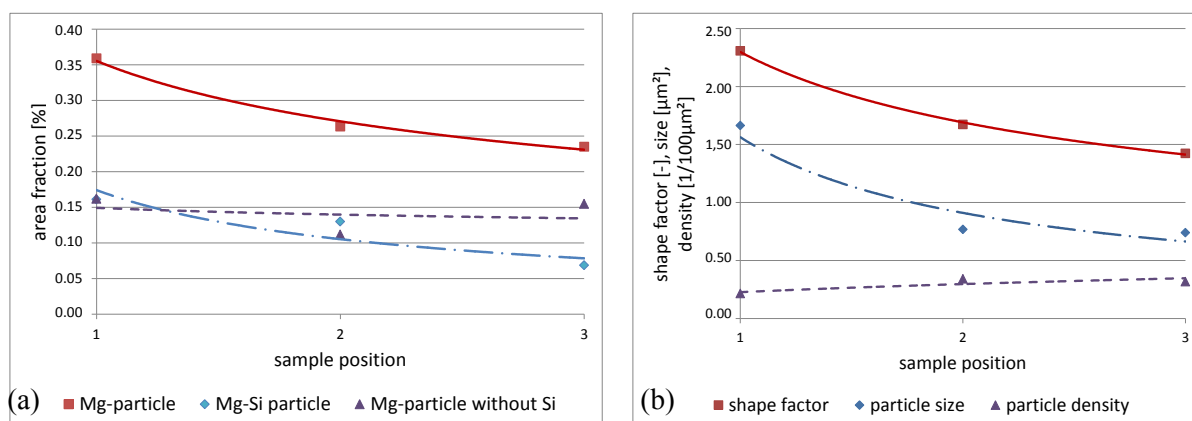


**Figure 2.** Evaluation of feature analysis with respect to the characteristics of Mg-bearing particles with and without Si along the sample arm.

### 4.2. Results of simulations

The results of the thermodynamic calculations in figure 3 show that for cast-iron relevant temperatures MgO or MgS may form directly, as soon as Mg, O, and S are in the melt or at the free surface. The amounts of MgO at about 1780 °C and MgS at about 1700 °C arise due to the assumed oxygen or sulphur content of the melt. If the locally available oxygen and sulphur are depleted by reaction with magnesium, further reaction products such as  $\text{Mg}_2\text{C}_3$  can occur at lower temperatures. A further study varying the oxygen content shows that in the multi-component system Fe-C-Mg-Si-O, the oxygen content determines which magnesium compounds are stable before solidification starts. At a temperature of 1250 °C and oxygen content up to 0.03 wt.-% in the full equilibrium liquid magnesium and magnesium oxides are expected.

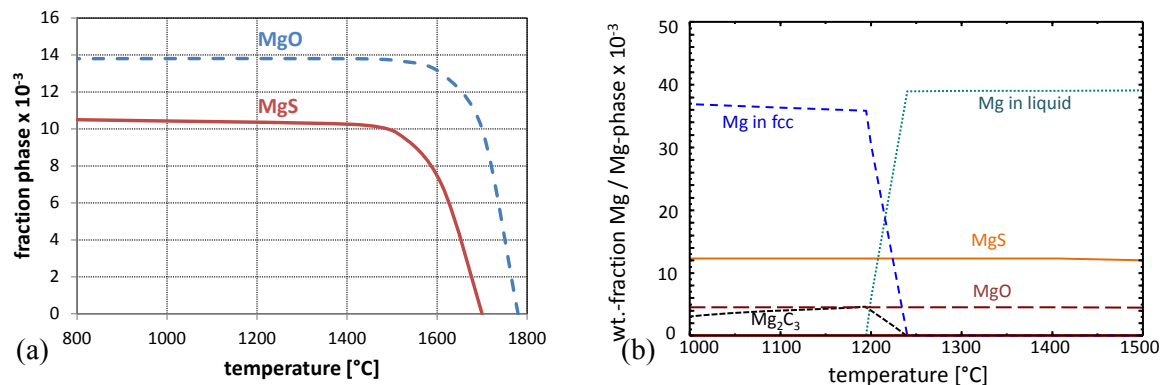


**Figure 3.** Weight fractions of MgO and MgS calculated with FactSage (a) and of Mg-bearing phases based on the composition given in Section 3.1 without Mn and P (b).

The microsegregation simulation showed a significant enrichment of magnesium in the melt on solidification. Calculations were performed based on the same melt concentration varying the retained magnesium content: 0.02, 0.04, 0.08 wt.-%. These calculations resulted in the following concentrations at 1 wt.-% liquid phase: Fe C3.96 Si1.2 Mn0.29 and Mg 0.21, 0.43, 0.87 wt.-% respectively.

With these concentrations subsequent equilibrium calculations with FactSage [8] were performed. The results of these calculations with respect to the formation of MgO and Mg<sub>2</sub>C<sub>3</sub> are shown in figure 4. After the residual oxygen is consumed, Mg<sub>2</sub>C<sub>3</sub> may form at the given composition at about 1260°C. The amount of Mg<sub>2</sub>C<sub>3</sub> scales linearly with the concentration of the residual liquid, which the results of Sofue et al. [1] confirm. In summary, the formation of silicate inclusions is to be expected at higher oxygen concentrations such as surface contact, and at lower oxygen concentrations MgO, MgS, or Mg<sub>2</sub>C<sub>3</sub> can be formed. This does not exclude the formation of complex compounds that were not included in the databases or due to other reactants such as P, S, Ca, Ce.

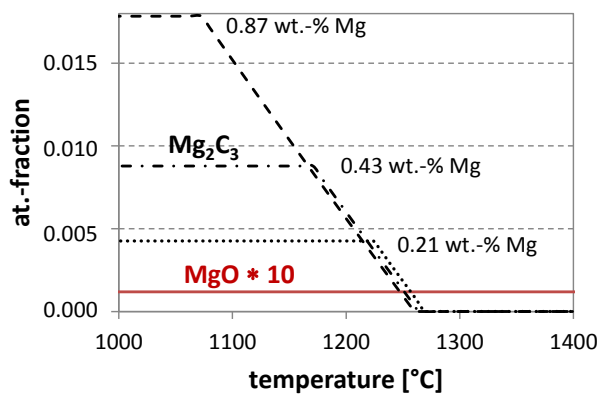


**Figure 4.** FactSage calculations with the databases Iron-01c [10] and FToxid [8]. Phase fractions for varying magnesium concentrations of the residual liquid: 0.21, 0.43, 0.87 wt.-%, and 19 ppm oxygen. The initial retained magnesium content of the melt was 0.02, 0.04, and 0.08 wt.-%.

## 5. Summary and conclusions

The thermodynamic results indicate that a reaction of magnesium and oxygen already takes place above the liquidus temperature leading to the formation of MgO and, at higher concentrations of oxygen, also to the formation of magnesium silicates. Smaller magnesium silicates can thus arise, for example during mold filling in surface contact and then pass into the cast component. The remaining magnesium segregates and reacts at a sufficient concentration with the segregating elements oxygen and sulphur, until they are fully consumed. According to the calculations Mg<sub>2</sub>C<sub>3</sub> is following. The

influence of the oxygen concentration on the reaction equilibria indicates that during the Mg treatment at first magnesium silicates form.

The amount of the non-Si-bearing precipitates remained approximately constant in each sample, whereas particle number and size varied greatly. This observation supports the precipitation hypotheses for non-Si-bearing Mg inclusions. All results and analyses of the present study suggest that non-metallic inclusions, such as Mg (O, C, S, N, P) only form during solidification by segregation as precipitates. Astonishingly, the amount of Si-bearing inclusions decreased. This observation contradicts the inclusion hypotheses because more surface contact due to vortices developing behind the three flow obstacles does not increase the amount of magnesium silicates as expected. This means that no significant amount of Si-bearing particles is formed on mold filling; these particles must be pre-existing. The pre-existing particles may be trapped in the flow shadow of the flow obstacles and decrease therefore. The overall decrease in the size and proportion of Mg-bearing particles as well as the improvement of the form factor lead to the conclusion that vortex formation may have a positive impact on fatigue strength. This has to be further investigated.

The literature review shows that all particles near the grain boundaries weaken the grain boundaries under stress, even with rounded shape, which is why these are undesirable together with carbides also caused by segregation. The avoidance of Mg-bearing precipitates is possible in SGI only in so far as that the optimal retained Mg content of 0.06 wt.-% should not be exceeded. At higher retained Mg contents, the effect of grain boundaries weakened by non-metallic precipitates outweighs the effect of improved particle roundness. Sofue et al. [1] show the relationships between retained Mg content, nonmetallic inclusions, graphite mold and matrix hardness on the fatigue strength. On this basis, they developed criteria for optimal properties.

### Acknowledgment

The research project 16698 N / 1 of the Research Association for Foundry Technology e.V. (FVG) was sponsored by the AiF under the programme for the promotion of industrial research and development (IGF) by the Federal Ministry of Economics and Technology based on a decision of the German Bundestag and professionally supervised by the Federal Association of German Foundry Industry (BDG). For the support of this work we thank the agencies involved cordially. Also, we thank the participants of the accompanying working group, in particular the DOSSMANN GmbH, Wallduern-Rippberg and SHW Casting Technologies GmbH, Aalen-Wasseralfingen.

### References

- [1] Sofue M, Okada S and Sasaki T 1979 *AFS Trans.* **87** 173
- [2] Horie H, Kowata T, Onisawa H and Shindo Y 1987 *J. Japan Foundrymen's Society* **59** 302
- [3] Lin H M, Lui T S and Chen L H 2003 *Mat. Trans.* **44** 1209
- [4] Schneider A 2006 *Salzgitter-Mannesmann Aktuell* 2
- [5] Wiener J, Gigacher G, Penz S and Bernhard C 2009 *Berg- und Hüttenmännische Monatshefte* **154** 33
- [6] Obermaier S, Kleiner S, Zeipper L and Kauffmann M 2009 *Gießtechnik im Motorenbau*. VDI- Bericht 2061
- [7] Andersson J, O Helander T, Höglund L, Shi P F and Sundman B 2002 *Calphad* **26** 273
- [8] Bale CW, Bélisle E, Chartrand P, Deckerov SA, Eriksson G, Hack K, Jung IH, Kang YB, Melançon J, Pelton DA, Robelin C and Petersen S 2009 *Calphad* **33** 295
- [9] Gagne M, Paquin M P and Cabanne P M 2008 *Ductile Iron Society T&O Meeting* 142
- [10] Pustal B, Subasic E, Hallstedt B, Schäfer W, Bartels C, Siebert H, Schneider J M and Bührig-Polaczek A 2010 *Adv. Eng. Mat.* **12** 158